in vivo *26*: 619-626 (2012)

Imaging EGFR Phosphorylation in Intact Human Pancreatic Carcinoma Cells

R. MAGDEBURG[1], M. KESSLER[1], R. BOENNINGHOFF[1] and M. KEESE[1,2]

[1]*Department of Surgery, University Medical Centre Mannheim, Medical Faculty Mannheim of the University of Heidelberg, Mannheim, Germany;*
[2]*Clinic for Vascular and Endovascular Surgery, Johann Wolfgang Goethe University Hospital, Frankfurt, Germany*

Abstract. *Background/Aim: Carcinoma of the pancreatic duct is a highly malignant tumor characterized by aggressive and early metastastatic growth. A high rate of tumor recurrence after surgical resection and the lack of effective chemotherapeutic approaches result in low 5-year survival rates. Overexpression of epidermal growth factor (EGF) and its receptor have been correlated to a higher tumor biological aggressiveness. Materials and Methods: We investigated EGFR RNA and protein expressions in different pancreatic carcinoma cell lines. EGFR phosphorylation was determined using acceptor photobleaching fluorescence resonance energy transfer (FRET). Results: The imaging method allowed determination of receptor phorphorylation in intact cells without external calibration. Significant differences between the cell lines were found in EGFR expression but not in phosphorylation of EGFR without EGF stimulation. After stimulation with EGF, significant differences were found in receptor phorphorylation. EGFR expression did not correlate with EGFR phorphorylation. Conclusion: Since EGFR phosphorylation conveys signal transduction within cells, this molecular imaging method could be useful for the identification of patients with a high level of EGFR phosphorylation within tumor cells and, thus, to select patients for an EGFR-targeted therapy.*

Pancreatic cancer is the fourth leading cause of cancer death in the United States and the sixth in Europe (1, 2). Most patients with pancreatic cancer are diagnosed with a late stage in the progression of the disease and have only a few months to live (3). Although cytotoxic chemotherapies have been extensively studied in advanced cancer, historically they have provided only modest benefits (4-6). Five-year survival has improved significantly over time only in patients with resectable tumors (7). Earlier diagnosis and better patient selection explain the better outcome. In patients with unresectable tumors, the 5-year survival rate was 3% in 1970; more than 20 years later, it had improved to only 4% (3). Chemotherapy is unlikely to substantially alter the natural history of pancreatic cancer, a disease refractory to most cytotoxic agents. Only gemcitabine has become the standard therapy in the adjuvant or palliative setting (8, 9). The reasons for the aggressive growth and metastatic behavior of pancreatic cancer are still poorly understood.

Many epithelial tumor entities including gastric and cervical cancer, as well as cancer of the head, neck, breast and lung, express high densities of the epidermal growth factor receptor (EGFR). Upon ligand binding, EGFR dimerizes, leading to receptor phosphorylation on multiple tyrosyl residues catalyzed by its intrinsic tyrosine kinase activity. These phosphorylated tyrosyl residues recruit proteins with SRC homology-2 and phosphotyrosine binding domains, thereby assembling multiprotein complexes which propagate the signal inside the cell (10). These complexes induce the Notch-1 - Furin interaction. This is a well-regulated process which achieves cross talk between the SRC and Notch signaling pathways (11).

The number of phosphorylated receptors is determined by the balance between tyrosine kinase and specific protein tyrosine phosphatase (PTP) activities (12). Overexpression or co-expression of EGFR and its ligands is associated with advanced stage and reduced survival in pancreatic cancer patients (13, 14). The EGFR is overexpressed in approximately 90% of pancreatic cancer cases (13). Up-regulation and overexpression of the EGFR has been correlated to many processes related to cancer, including uncontrolled cellular proliferation, autocrine stimulation of tumors producing their own growth factors (*e.g.* TGF-β, EGF) and prevention of

Correspondence to: R. Magdeburg, MD, Department of Surgery, University Medical Centre Mannheim, Medical Faculty Mannheim of the University of Heidelberg, 68167 Mannheim, Germany. Tel: +49 6213832357, e-mail: richard.magdeburg@umm.de

Key Words: EGFR, pancreatic carcinoma, imaging, CAPAN1, HPAC, HUVECs cells.

Table I. *Cell lines used in this study.*

Cell line	Origin	Provider	Grading	Known EGFR expression
PATU 8988	Human pancreatic carcinoma	DSMZ	G2-3	–
PATU 8902	Human pancreatic carcinoma	DSMZ	G2-3	–
CAPAN 1	Human pancreatic carcinoma	DSMZ	G2	++
HPAC	Human pancreatic carcinoma	ATCC	G2	++
Fibroblasts	Dermis	University hospital Mannheim		++
HUVEC	Human umbilical vein	University hospital Mannheim		+

– Expression unknown, + moderate expression, ++ high expression.

apoptosis (15-17). This also appears to protect cancer cells from the toxic actions of chemotherapy and radiotherapy, rendering these treatment modalities less effective.

The expression level of the receptor is not necessarily an indicator of its signaling activity in tumor cells. High expression levels for EGFR do not necessarily indicate a high level of intracellular EGFR activity. Particularly in view of the novel EGFR-targeting treatment modalities, we have developed a method for direct imaging of endogenous EGFR phosphorylation in tumor cells (18). To better characterize the role of EGFR in pancreatic carcinoma, here we investigated EGFR expression and EGFR phosphorylation within human pancreatic carcinoma cells, HUVECs and fibroblasts (Table I).

Materials and Methods

Reagents. Human recombinant EGF was purchased from Calbiochem™ (San Diego, Ca, USA). Vanadate was obtained from Sigma-Aldrich™ (Taufkirchen, Germany). Cell culture materials were obtained from Invitrogen™ (Carlsbad, Ca, USA). EGFR antibodies binding to the sequence DVVDADADEYLIPQ which corresponds to the amino acid residues 985-996 (referred to as F4) and generic phosphotyrosine antibodies (referred to as PY72) were obtained from the monoclonal cell facility of Cancer Research UK (London, UK). Monoreactive dyes Cy3 and Cy5 were purchased from Molecular Probes, Inc. (Eugene, OR, USA).

Cell culture. The cell line HPAC was provided by the American Type Culture Collection (ATCC, Rockville, MD, USA); the cell lines PATU 8988S, PATU8902 and CAPAN 1 were provided by the German Collection of Microorganism and Cell Cultures (DSMZ, Braunschweig, Germany). HUVECs and fibroblasts were isolated and cultured at the Surgical Laboratory of the University Hospital Mannheim. They were maintained in MEM (PATU8988S, PATU8902, HPAC), RPMI (CAPAN1, fibroblasts) or Endopan (HUVECs) medium supplemented with 5-20% (v/v) heat-inactivated fetal bovine serum, 100 UI/ml penicillin, 100 μg/ml streptomycin and 1% (v/v) glutamine (ICN, Irvine, UK) in a humidified atmosphere of 95% air and 5% CO_2 at 37˚C. Stock cultures were stored in liquid nitrogen and used for experimentation within five passages. Cell viability was assessed by trypan blue dye exclusion before cells were processed further.

Cells were grown to 70% confluency in 6-well dishes containing glass cover slips. Cells were starved (1% FCS) for 24 h and then exposed to EGF (100 ng/ml) or pervanadate (final concentration of 1 mM after oxidization of vanadate by addition of 30% H_2O_2 to the 200 mM stock solution). Controls received the carrier (PBS). After incubation, cells were fixed in 4% paraformaldehyde for 20 minat room temperature and permeabilized with 0.1% Triton X before staining.

Antibody labeling. F4 antibody binding a conserved intracellular domain of EGFR was labeled with Cy3. Antiphosphotyrosine antibody PY72 binding was labeled with Cy5. For labeling, 10 μl aliquots of 1 M Na-Bicine buffer, pH 9.0 were added to 90 μl antibody solution in PBS and a 20 fold molar excess of the monofunctional N-hydoroxysuccinimidyl-ester of the chromophores was added from a 10 mM stock solution in N, N-dimethylformamide (DMF). Conjugation reactions were allowed to proceed for 40 min in the dark, at room temperature. Labeled antibody was separated from free un-reacted dye by gel exclusion chromatography using Econo-Pac 10DG columns (BioRad™, Hercules, CA, USA), and concentrated to 1 mg/ml using Centricon centrifugal filter devices (Millipore, Bedford, MA, USA). The dye/protein labeling ratio was determined to be ~5 chromophores per antibody by absorption spectroscopy. Fixed, permeabilized cells were incubated with 3 μg/ml F4-Cy3 and 9 μg/ml PY72-Cy-5 in PBS containing 1% bovine serum albumin (BSA) for 2 h at 37˚C in a moist chamber. The stained cells were then washed five times with PBS and mounted on a glass slide in Mowiol (Calbiochem™, San Diego, CA, USA).

FRET-microscopy. For acceptor photobleaching FRET imaging a confocal laser scanning Leica SP2 microscope (Leica™, Bensheim, Germany) was used. All measurements were obtained using a ×63/1.32 NA objective. Simultaneous images with the pinholes set at two Airy units were acquired from donor (Cy3) and acceptor (Cy5), using 10% of the maximal 554 nm HeNe laser line power for excitation of Cy3 and 15% of the 633 nm laser line power for excitation of Cy5. Detection of fluorescence was in the spectral window of 560-595 nm for Cy3 and 650-700 nm for Cy5. Acceptor photobleaching was performed by irradiation of Cy5 in a region of interest (zoom=25) with the 633 nm laser line set at maximum intensity for eight rounds with a line average of four. Post-bleached donor (Cy3) images were acquired by reverting back to the original acquisition settings. The FRET efficiency (E) was calculated by normalizing the difference of the donor post- and pre-bleach intensities by the post-bleach intensity according to (18):

$$E=(I_{postbleach} - I_{prebleach})/I_{postbleach}.$$

Control samples labeled with the donor (Cy3) and acceptor (Cy5) alone were used to verify that no bleed-through of acceptor fluorescence was present in the donor channel disturbing the calculation of the FRET efficiency at the used spectral settings. All acquired images were transferred to a Leica NT work station. Image processing was performed using the ScionImage beta 4.2 software (Scion Corporation™, Frederick, MD, USA). Difference images were obtained with IP-Lab version 3.5.5 (Scananalytics™, Fairfax, VA, USA).

RNA isolation. A total of 5×10^6 cells were lysed with 1 ml Trizol (Invitrogen™, Carlsbad, CA, USA). After adding 0.2 ml chloroform and mixing for 3 min, the suspension was centrifuged at 12000 ×*g* for 15 min at 4˚C. A second extraction with phenol/chloroform was performed, followed by an isopropanol precipitation. Total RNA samples containing pellets were air dried, dissolved in water and purity was determined by gel electrophoreses. Samples were treated with DNAse before storage at –80˚C.

RT-PCR for EGFR. cDNA was derived by a reverse-transcriptase reaction with AMV-PT and Oligo-p(dT)-primers (25˚C 10 min, 42˚C 1 h, 95˚C 5 min, cooling to 4˚C). An EGFR-specific primer pair designed by Tib Molbiol Syntheselabor™ (Berlin, Germany) was used for amplification in a T-gradient cycler (Biometra™, Göttingen, Germany): 5' TCT CAG CAA CAT GTC GAT GG 3', 5' TCG CAC TTC TTA CAC TTG CG-3'. PCR conditions were as follows: 94˚C 2 min, 38 cycles 94˚C 30 s, 66˚C 45 s, 72˚C over 45 s with a final elongation time of 10 min. PCR products were analyzed on a 2% agarose gel.

Cloning a standard for EGFR. An RNA standard was cloned from the 474 base pair PCR fragment. In brief, PCR fragments were purified according to the QIAquick PCR purification kit (Qiagen™, Hilden, Germany). Then 50 ng of the purified fragment were incubated with 50 ng of pDRIVE cloning vector for 10 min. Ligation mix was added. 50 µl bacteria were co-incubated with 2 µl plasmid solution in (SOC) medium and heat shocked (42˚C, 30 s). The transformation mixture was plated on ampicillin-containing (LB) agar dishes for overnight culture. (X-Gal) negative clones were derived and amplified in 15 ml medium. Plasmids were isolated with the QIAprep Miniprep kit (Qiagen™). The length of the plasmids was determined by gel electrophoresis and then the sequence was determined (Sequlab™, Göttingen, Germany). For *in vitro* transcription, plasmids were treated with AVRII (2 IU/µg plasmid, 37˚C, 60 min) before incubation with RNA polymerase T7. RNA was purified as described above.

Real time PCR. Kinetic RT-PCR was performed with a LightCycler (Roche Diagnostics™, Mannheim, Germany) by using SYBR Green I as a double-strand DNA-specific binding dye. Since the EGFR primer pair used for the cloning step described above exhibited dimer formation in the melting curve analysis, a different EGFR-specific primer pair coding for a 217 base pair fragment of EGFR cDNA contained within the region of EGFR, used as 474 base pair standard, was used. Primers used for the LightCycler PCR were designed by Tib Molbiol Syntheselabor™ (Berlin, Germany): 5'-GAG GAG AAC TGC CAG AAA CTG A-3' and 5'-GGT ACG TGG TGG GGT TGT AGA-3'. The following single-step RT-PCR protocol was used for detection: amplification was carried out in a total volume of 20 µl in glass capillaries containing 0.5 µM of each primer, 3.25 µM $Mn(Oac)_2$, 2 µl Light Cycler RNA Master SYBR Green I (containing Tth Polymerase, 10 × Taq buffer, 2 mM of each dNTP, SYBR Green I; Roche Diagnostics™) and 10 ng RNA diluted in 2 µl. All RNA samples were tested for their RNA concentration by photometry. RT was performed at 50˚C for 20 min. Probes were denaturated at 95˚C over 15 min. Amplification conditions were 95˚C for 15 s, 52˚C for 20 s, 72˚C for 15 s, 10 s with temperature transition rate of 20˚C/s with acquisition at 80˚C. Additionally for control, the PCR product was visualized after agarose gel electrophoresis.

ELISA. Levels of full length-EGFR protein were measured using the KHR 9061 ELISA kit (Biosource International™, Camarillo, CA, USA). Phosphorylated EGFR protein (Tyrosine 1173) levels were measured using the KHR 9071 ELISA kit (Biosource International™). Assays were performed in duplicate using 200 µl per well in accordance with the manufacturer's instructions. Cells were trypsinized, resuspended in PBS and proteins were extracted by incubation in cell extraction buffer (Biosource International™) for 30 min at 0˚C. Samples were centrifuged at 10000 ×*g* for 10 min and the protein concentration in the supernatant was determined using a BCA protein assay. Samples used for ELISA contained 30-40 mg/ml protein. Values were read on a DPC™ (Los Angeles, CA, USA) microplate spectrophotometer at 450 nm.

Statistics. The data were analyzed for statistical significance with the Students–*t*-test using the SPSS™, (Chicago, IL, USA) software package. *p*-Values of <0.05 were considered significant. In the box blots used for graphical data representation, a box is drawn around the interquartile range; a line inside the box indicates the median value; error bars are drawn at the 5% and the 95% confidence intervals.

Results

High EGFR expression in tumor cells has been discussed in several earlier studies. The EGFR expression levels reported for specific tumors in the literature vary widely from study to study. EGFR RNA expression was found in all investigated cell lines; the expression in tumor cell lines was significantly higher than in non-malignant cell lines. The highest number of *EGFR* mRNA copies were found in undifferentiated PATU 8902 and PATU 8988S cells, while the better-differentiated HPAC and CAPAN1 cells had intermediate levels of EGFR RNA expression slightly higher then the expression in non-malignant cell lines (Figure 1a). Basal protein expression in starved cells, as determined by ELISA, generally correlated with the expression levels derived for mRNA. The highest levels of EGFR protein were found in PATU 8902 and PATU 8988S cells (Figure 1b).

A fast and easy way to determine EGFR phosphorylation is by ELISA measurements at the phosphorylation level of a single tyrosine residue (tyrosine 1173). Again, in starved cells, the levels of *EGFR* mRNA and EGFR protein generally correlated to the level of EGFR phosphorylation (Figure 1c). Inhibition of EGFR dephosphorylating phosphatases by vanadate is expected to give maximal levels

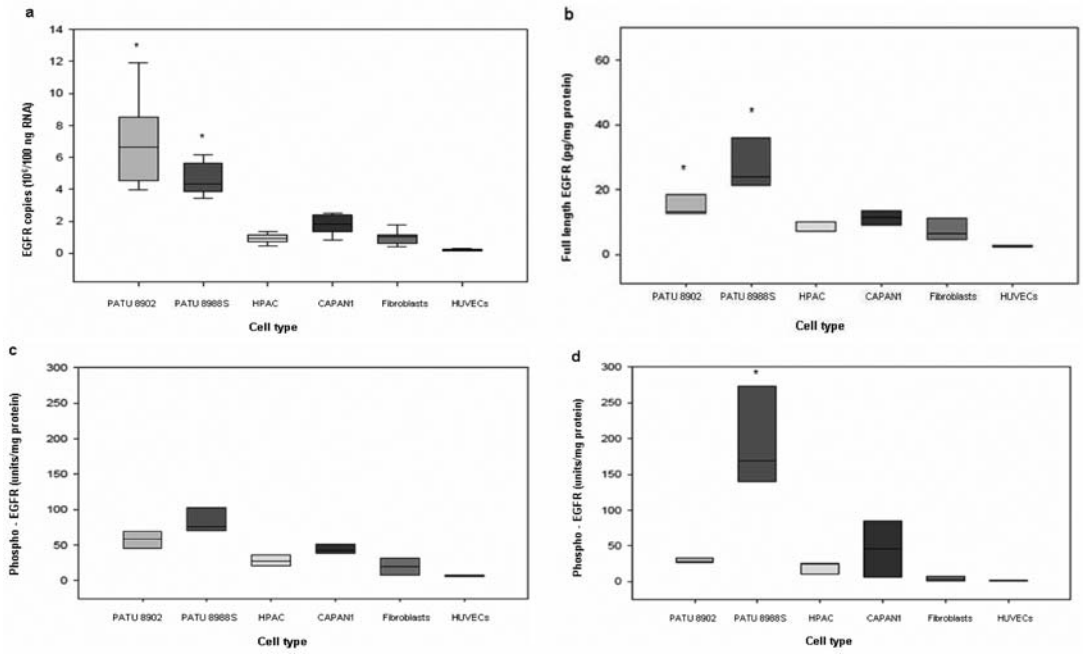

Figure 1. *EGFR expression and phosphorylation. Data from 15 independent RNA or protein extractions are shown. a: EGFR RNA levels as determined by light cycler PCR; 100 ng of RNA were analyzed. b: EGFR protein levels as determined by full-length ELISA. c: EGFR phosphorylation at Tyr 1173, as determined by ELISA after serum starvation for 24 hours. d: EGFR phosphorylation at Tyr 1173, as determined by ELISA after 20 min of stimulation with vanadate. (*p<0.05).*

of EGFR. After inhibition of EGFR dephosphorylating phosphatases, the levels of EGFR protein was not significantly different from that of starved cells, at all cell lines (data not shown). But even with maximal EGFR phosphorylation by vanadate, there was an increase in the level of phosphorylated tyrosine 1173 in one single cell line, PATU 8988 (Figure 1d).

FRET was used to monitor phosphorylation levels in the cells. Detection of the co-occurrence of a specific Cy3 tagged anti-EGFR antibody and a generic Cy5-coupled anti-phosphotyrosine antibody on EGFR by FRET allows a highly specific quantification of EGFR phosphorylation in cells. Here, EGFR phosphorylation at all tyrosine residues was imaged by this two-antibody FRET approach using acceptor photobleaching. The data from a typical FRET experiment are shown in Figure 2.

Using this optical assay, we characterized and compared EGFR activity in the different cell lines. To determine the degree of autonomous EGFR autophosphorylation in these cells lines, all cells were serum starved for 24 hours before imaging experiments. The starved cell lines exhibited low autonomous EGFR activity in the FRET experiments, with there being no significant differences between the single cell lines (Figure 3a). Maximal EGFR phosphorylation by vanadate should occur even in the absence of exogenous ligands due to the basal kinase activity of EGFR. All cells responded well to vanadate treatment and showed a significant increase in FRET efficiency in relation to the basal activity (Figure 3b). The maximum FRET efficiency was lower in the non-malignant cells (fibroblasts). EGF stimulation led to an increase in EGFR phosphorylation over time with a maximum being reached after 20 min (data not shown). Therefore starved cells were stimulated by EGF for 20 min and fixed thereafter for the FRET measurements. After EGF stimulation all cells exhibited an increase in FRET efficiency ($p<0.05$, Figure 3c), as compared to the level of basal phosphorylation. Only in fibroblasts did EGFR remain low after stimulation.

Discussion

Activation of the EGFR has been shown to contribute to the growth and spread of many different types of solid tumor. The receptor appears to protect cancer cells from the toxic actions of chemotherapy and radiotherapy, rendering these treatments less effective. Up-regulation and overexpression of the EGFR has been correlated to many processes related to cancer (15-17).

Many epithelial tumors express high EGFR densities, which are associated with advanced disease and poor clinical prognosis (13). Therefore multiple attempts have been made to target EGFR by antitumoral therapy in patients with

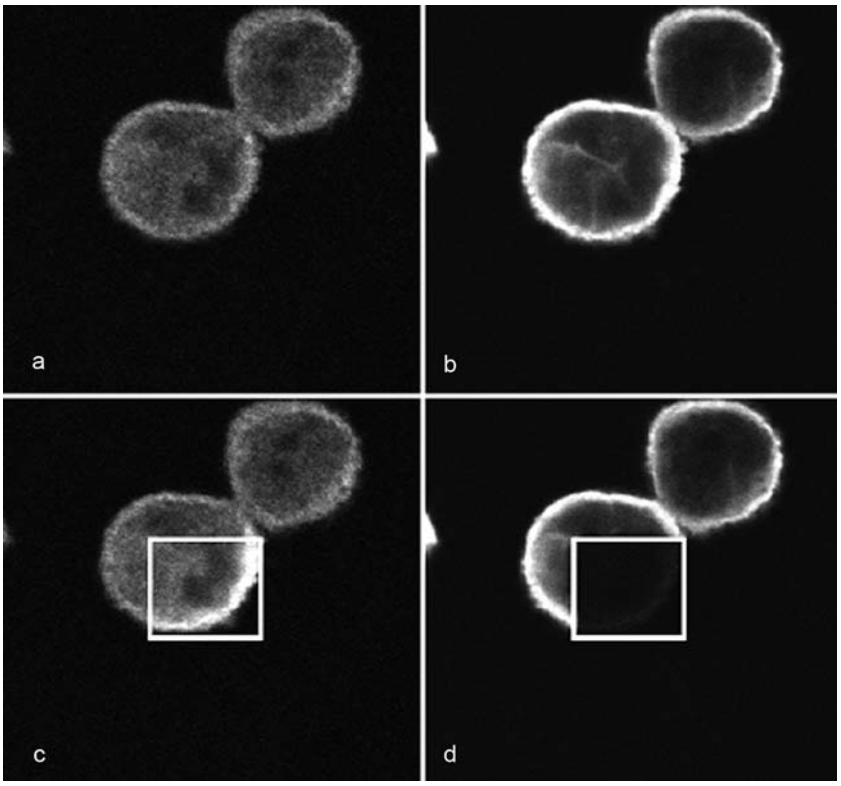

Figure 2. *EGFR phosphorylation as determined by acceptor photobleaching FRET. a: F4-Cy3 donor signal before photobleaching. Donor fluorescence is reduced by FRET. b: Corresponding Py72-Cy5 fluorescence in the same cells before photobleaching. c: F4-Cy3 donor signal after bleaching of Cy5. An increase of fluorescence can be identified within the bleached area. d: Py72-Cy5 acceptor signal after bleaching of Cy5.*

pancreatic carcinoma. Although different pancreatic carcinoma cell lines exhibited a pronounced *in vitro* response to tyrosine kinase inhibitors of EGFR (19, 20), only a small number of patients seem to profit from this therapy (21).

We therefore determined EGFR expression in the pancreatic carcinoma cell lines PATU 8902, PATU 8988S, CAPAN 1 and HPAC, and in non-malignant cells (HUVECs and fibroblasts). EGFR RNA and protein expression was found in all cells. EGFR RNA levels correlated well with the amount of protein expression. The EGFR expression in tumor cell lines was significantly higher than that in HUVECs and fibroblasts. While the better-differentiated HPAC cells had an intermediate level of EGFR expression, the undifferentiated PATU 8902 and PATU 8988S cell lines had the highest levels of *EGFR* mRNA. If injected into nude mice, both these cell lines develop metastases with low differentiation. This underlines that when isolated from tumor, cells represent not the whole tumor entity but only a small proportion of the cells present in the tumor.

No correlation has yet been found between the level of EGFR expression and the prognosis of different tumor entities (22, 23). The transduction of EGFR signaling inside the cell depends on multiple variables. Upon ligand binding, EGFR dimerizes which leads to receptor activation and the phosphorylation of multiple tyrosyl residues. These tyrosyl residues recruit proteins with SRC homology 2 and phosphotyrosine binding domains, thereby assembling multiprotein complexes, which propagate the signal. The amount of phosphotyrosines is determined by the balance of EGFR activity and the activity of PTPs (12); *e.g.* PTP1B is a widely expressed, prototypical nontransmembrane phosphatase, which dephosphorylates numerous receptor tyrosinekinases, including the EGFR. Interaction of EGFR with the catalytic center of PTP1B leads to receptor dephosphorylation, which requires receptor endocytosis and takes place at discrete locations inside the cell (24).

As a fast and easy way to determine EGFR phosphorylation, ELISA measurements that determine the phosphorylation state of the single tyrosine residue, tyrosine 1173, have been proposed. Several other tyrosine residues have been found which are equally important for autophosphorylation of EGFR (25). The level of phosphotyrosine 1173 correlated to the level of *EGFR* mRNA and EGFR protein in starved cells. Protein levels remained

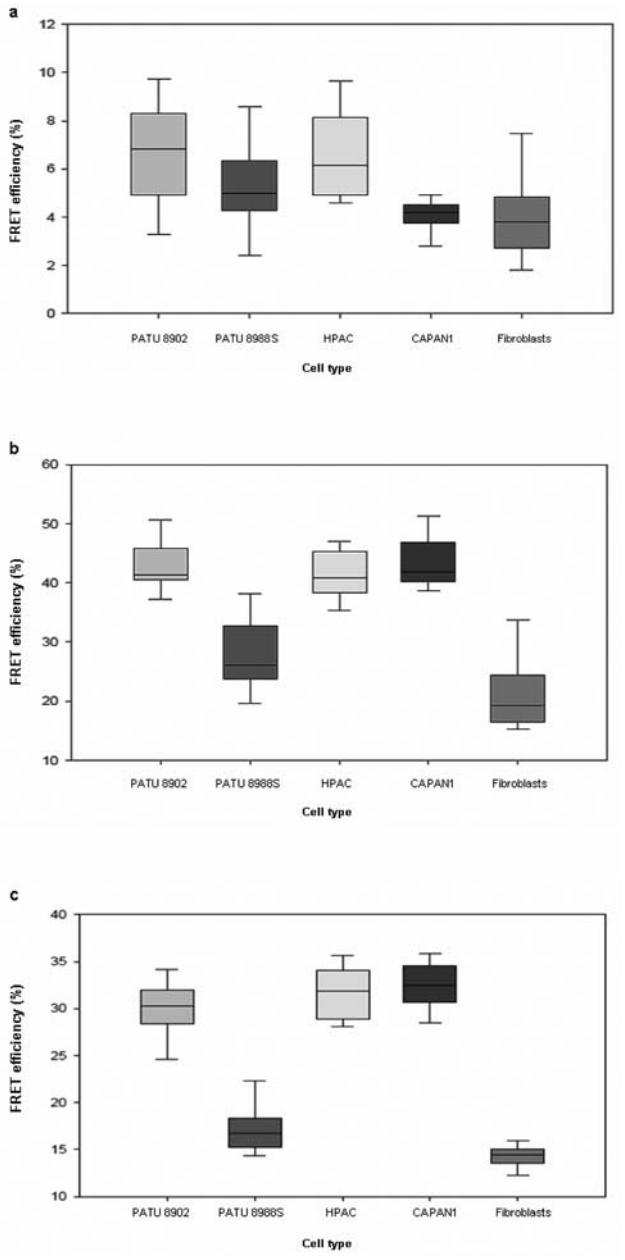

Figure 3. *EGFR phosphorylation as determined by FRET efficiency (n=30; cells were photobleached in three different preparations: after serum starvation for 24 hours (a), 10 min after stimulation with vanadate (b), and 20 min after EGF stimulation (c).*

unchanged when the cellular phosphatases were inhibited by vanadate. Interestingly this led to an increase of phosphorylated tyrosine 1173 in only one single cell line (PATU 8988). This underlines that the level of tyrosine 1173 phosphorylation is not a reliable indicator of EGFR activity. In spite of enhanced EGFR signaling, a reduced rate of tyrosine 1173 phosphorylation may be found (26).

In the search for alternative ways to determine EGFR phosphorylation, we previously developed a FRET assay (18). Spatially resolved FRET has provided a method for tracing the catalytic activity of fluorescently tagged proteins inside live cell cultures, which allows accurate measurement of EGFR phosphorylation (27-30). This FRET-based assay was previously used to monitor the EGFR activity in colon cancer cells (18). We here employed this assay in pancreatic tumor cells. Hereby, Cy-3 tagged antibodies (donor) to the F-4 domain of the EGFR and Cy-5 antibodies to phosphorylated tyrosine domain PY-72 were used. FRET was quantified by laser scanning confocal microscopy after photobleaching of the acceptor and by comparing donor intensities of the pre-bleach and post-bleach images. Unlike previous experiments in colorectal cancer cells (18), we only found a low rate of EGFR phosphorylation after serum starvation, probably confirming the presumption of a lack in receptor tyrosine-kinases-activating mutations in pancreatic carcinoma. Our experiments showed that the FRET-imaging assay can be used in a variety of cell lines. We furthermore showed that unlike ELISA assays, spatially resolve FRET assays convey a spatially resolved, accurate information of the EGFR posphorylation within intact single cells. We hereby showed that there is a cell type-specific, individual response in the level of EGFR phosphorylation after stimulation with EGF. In further studies, we will investigate if high FRET activity within tumor samples can be used to predict clinical response to EGFR inhibitors in patients with tumor.

Acknowledgements

This work was supported by the Paul Blümel Stiftung Hannover.

References

1 Malvezzi M, Bertuccio P, Levi F, La Vecchia C and Negri E: European cancer mortality predictions for the year 2012. Ann Oncol *23*: 1044-1052, 2012.

2 Krejs GJ: Pancreatic cancer: epidemiology and risk factors. Dig Dis *28* 355-358, 2010.

3 Ahlgren JD: Epidemiology and risk factors in pancreatic cancer. Semin Oncol *23*: 241-250, 1996.

4 Klinkenbijl JH, Jeekel J, Sahmoud T, van Pel R, Couvreur ML, Veenhof CH, Arnaud JP, Gonzalez DG, de Wit LT, Hennipman A and Wils J: Adjuvant radiotherapy and 5-fluorouracil after curative resection of cancer of the pancreas and periampullary region: phase III trial of the EORTC Gastrointestinal Tract Cancer Cooperative Group. Ann Surg *230*: 776-782, 1999.

5 Neoptolemos JP, Stocken DD, Friess H, Bassi C, Dunn JA, Hickey H, Beger H, Fernandez-Cruz L, Dervenis C, Lacaine F, Falconi M, Pederzoli P, Pap A, Spooner D, Kerr DJ and Buchler MW: A randomized trial of chemoradiotherapy and chemotherapy after resection of pancreatic cancer. N Engl J Med *350*: 1200-1210, 2004.

6 Reni M: Evidences and opinions for adjuvant therapy in pancreatic cancer. Curr Drug Targets *13*: 789-794, 2012.

7 Neuzillet C, Sauvanet A and Hammel P: Prognostic factors for resectable pancreatic adenocarcinoma. J Visc Surg *148*: e232-243, 2011.
8 Friberg G and Kindler HL: Chemotherapy for advanced pancreatic cancer: past, present, and future. Curr Oncol Rep *7*: 186-195, 2005.
9 Löhr J, Heinemann V and Friess H: Pankreaskarzinom Aktuelle Diagnostik und Therapie. UNI-MED 1. Auflage, 2003.
10 Zhang Q, Thomas SM, Xi S, Smithgall TE, Siegfried JM, Kamens J, Gooding WE and Grandis JR: SRC family kinases mediate epidermal growth factor receptor ligand cleavage, proliferation, and invasion of head and neck cancer cells. Cancer Res *64*: 6166-6173, 2004.
11 Ma YC, Shi C, Zhang YN, Wang LG, Liu H, Jia HT, Zhang YX, Sarkar FH and Wang ZS : the Tyrosine Kinase c-Src Directly Mediates Growth Factor-Induced Notch-1 and Furin Interaction and Notch-1 Activation in Pancreatic Cancer Cells. PLoS One. 2012; 7: e33414, 2012.
12 Flint AJ, Tiganis F, Barford D, and Tonks NK: Development of substrate-trapping mutants to identify physiological substrates of protein tyrosine phosphatases Proc Natl Acad Sci USA *95*: 1680-1685, 1995.
13 Salomon DS, Brandt R, Ciardiello F and Normanno N: Epidermal growth factor-related peptides and their receptors in human malignancies. Crit Rev Oncol Hematol *19*: 183-232, 1995.
14 Luo G, Long J, Qiu L, Liu C, Xu J and Yu X: Role of epidermal growth factor receptor expression on patient survival in pancreatic cancer: a meta-analysis. Pancreatology *11*: 595-600, 2011.
15 Waksal HW: Role of an anti-epidermal growth factor receptor in treating cancer. Cancer Metastasis Rev *18*: 427-436, 1999.
16 Wu X, Fan Z, Masui H, Rosen N and Mendelsohn J: Apoptosis induced by an anti-epidermal growth factor receptor monoclonal antibody in a human colorectal carcinoma cell line and its delay by insulin. J Clin Invest *95*: 1897-1905, 1995.
17 Mendelsohn J: The epidermal growth factor receptor as a target for therapy with antireceptor monoclonal antibodies. Semin Cancer Biol *1*: 339-344, 1990.
18 Keese M, Magdeburg RJ, Herzog T, Hasenberg T, Offterdinger M, Pepperkok R, Sturm JW and Bastiaens PI: Imaging epidermal growth factor receptor phosphorylation in human colorectal cancer cells and human tissues. J Biol Chem *280*: 27826-27831, 2005.
19 Bruns CJ, Harbison MT, Davis DW, Portera CA, Tsan R, McConkey DJ, Evans DB, Abbruzzese JL, Hicklin DJ and Radinsky R: Epidermal growth factor receptor blockade with C225 plus gemcitabine results in regression of human pancreatic carcinoma growing orthotopically in nude mice by antiangiogenic mechanisms. Clin Cancer Res *6*: 1936-1948, 2000.
20 Overholser JP, Prewett MC, Hooper AT, Waksal HW and Hicklin DJ: Epidermal growth factor receptor blockade by antibody IMC-C225 inhibits growth of a human pancreatic carcinoma xenograft in nude mice. Cancer *89*: 74-82, 2000.
21 Moore MJ, Goldstein D, Hamm J, Figer A, Hecht JR, Gallinger S, Au HJ, Murawa P, Walde D, Wolff RA, Campos D, Lim R, Ding K, Clark G, Voskoglou-Nomikos T, Ptasynski M and Parulekar W: Erlotinib plus gemcitabine compared with gemcitabine alone in patients with advanced pancreatic cancer: a phase III trial of the National Cancer Institute of Canada Clinical Trials Group. J Clin Oncol *25*: 1960-1966, 2007.
22 Gansauge F, Gansauge S, Schmidt E, Muller J and Beger HG: Prognostic significance of molecular alterations in human pancreatic carcinoma-an immunohistological study. Langenbecks Arch Surg *383*: 152-155, 1998.
23 Xiong HQ: Molecular targeting therapy for pancreatic cancer. Cancer Chemother Pharmacol *54(Suppl 1)*: S69-77, 2004.
24 Haj FG, Verveer PJ, Squire A, Neel BG and Bastiaens PIH: Imaging sites of receptor dephosphorylation by PTP1B on the surface of the endoplasmatic reticulum. Science *295*: 1708-1711, 2002.
25 Ullrich A and Schlessinger J: Signal transduction by receptors with tyrosine kinase activity. Cell *61*: 203-212, 1990.
26 Saito T, Okada S, Ohshima K, Yamada E, Sato M, Uehara Y, Shimizu H, Pessin JE and Mori M: Differential activation of epidermal growth factor (EGF) receptor downstream signaling pathways by betacellulin and EGF. Endocrinology *145*: 4232-4243, 2004.
27 Bastiaens PIH and Squire A: Fluorescence lifetime imaging microscopy: spatial resolution of biochemical processes in the cell. Trends Cell Biol *9*: 48-52, 1999.
28 Förster T: Delocalized excitation and excitation transfer. *In*: Modern Quantum Chemistry. Sinanoglu O, ed., Vol. 3, 93-137. Academic Press, New York, 1965.
29 Streyer L: Fluorescence energy transfer as spectroscopic ruler. Annu Rev Biochem *47*: 819-846, 1978.
30 Lakowicz JR: Principles of Fluorescence Spectroscopy, 2nd ed. Plenum, New York, 1999.

Received April 22, 2012
Revised June 12, 2012
Accepted June 13, 2012